J. Fluid Mech. (1979), *vol.* 95, *part* 4, *pp.* 635–653
Printed in Great Britain

Viscous flow through unsteady symmetric channels

By P. W. DUCK

Department of Mathematics Imperial College, London, S.W. 7†

(Received 24 October 1977 and in revised form 27 March 1979)

The high-Reynolds-number (K) flow through a symmetric channel, with walls whose shape is time dependent, is studied. The distortion of the walls is of non-dimensional height $O(K^{-\frac{1}{3}})$ and length $O(1)$, this particular size of perturbation being chosen such that (for the first regime of unsteadiness studied) the effects of the unsteadiness, viscous diffusion and advection all interact nonlinearly in the region of the fluid near the walls.

For this first regime of unsteadiness the problem is solved numerically. This leads on to analytic descriptions for progressively faster time variations of wall shape, and in fact the entire range of unsteadiness is covered for this particular size of distortion.

1. Introduction and statement of the problem

Much progress has been made recently in the study of steady, high-Reynolds-number flows past indentations or constrictions in channels and pipes. For instance, Smith (1976*a*) considered distortions of channel and pipe walls of slope lying between $O(K^{-1})$ and $O(K^{-\frac{3}{7}})$ for a non-symmetrical wall perturbation, or between $O(K^{-1})$ and $O(K^{-\frac{1}{3}})$ for a symmetrical distortion, K being the Reynolds number. Smith (1976*b*) went on to consider the two upper limits, $O(K^{-\frac{3}{7}})$ and $O(K^{-\frac{1}{3}})$, and later Smith (1977, 1978) considered still further parameter ranges for both symmetrical and non-symmetrical distortions; the distinction between symmetrical and non-symmetrical flows is a fundamental one, since in the latter case the core flow suffers no displacement, and consequently the perturbation in the core is of lower order than in corresponding non-symmetrical situations.

However, little progress has as yet been made with corresponding unsteady flows. The present work is an extension of that of Smith (1976*b*) to the high-Reynolds-number laminar flow of an incompressible fluid through a symmetrical channel, with walls whose shape is time dependent, the flow far upstream of the perturbation being steady and fully developed. Figure 1 shows the layout of the general situation.

This study has obvious applications in the physiological context, particularly to the problem of blood flow through flexible veins and arteries. In addition the analysis of flow through channels may have relevance in the study of flow through lung airways. There is evidence to suggest that precise distributions of flow velocity and rates of shear have considerable physiological importance, for conditions such as circulatory disease, however detailed flow distributions and shear rates are difficult to measure experimentally, and so there is a need for (reliable) theories to describe such flow quantities. But such a physical problem is a formidable mathematical one with the

† Present address: Department of Mathematics, University of Manchester, England.

0022-1120/79/4332-7710 $02.00

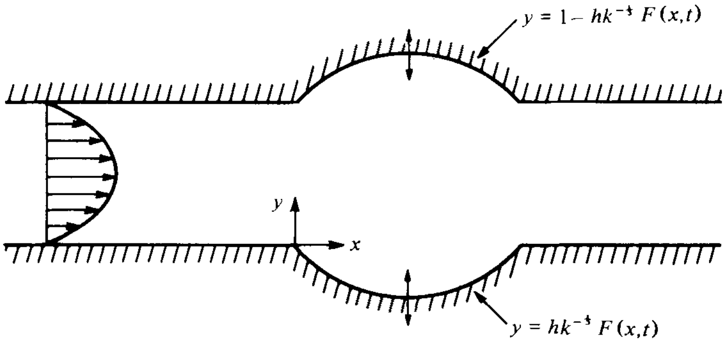

FIGURE 1. Layout of the problem.

combined difficulties of a pulsating basic flow, elastic and moving walls, branching, and even the possibility of non-Newtonian flow and turbulence. Consequently in this paper we focus our attention on just one of these problems, namely the effect of the unsteadiness of the wall on an otherwise steady oncoming Poiseuille flow.

q is the pressure gradient in the channel far upstream of any distortion, where the channel is straight and unperturbed, and here the flow is fully developed and steady, ν and ρ are the kinematic viscosity and density respectively, a is the undistorted channel width. Then we non-dimensionalize velocities and pressures with respect to $qa^2\rho^{-1}\nu^{-1}$ and aq respectively, ax and ay are taken as distances along and across the channel, and the indentations start at $x = 0$. The lower (unperturbed) wall lies along $y = 0$, whilst the upper (unperturbed) wall lies along $y = 1$.

The Reynolds number K is then defined by

$$K = qa^3/\rho\nu^2 \gg 1. \tag{1.1}$$

In this paper we shall assume throughout that the typical length of any perturbation is $O(1)$ on the x scale, and its non-dimensional height is $O(K^{-\frac{1}{3}})$, that is, we shall be concerned solely with 'fine' distortions of the channel. This particular size of distortion is chosen such that (for the first regime of unsteadiness considered), the effects of the unsteadiness, viscous diffusion and advection all balance near the walls, and so this particular size of perturbation is likely to be of most interest. Incidentally, in the steady case for this size of distortion the viscous and advective terms balance in the wall layer.

If a typical time scale is $1/\Omega$ (for an oscillatory wall motion, Ω would be the frequency of oscillation) then we non-dimensionalize time with respect to $1/\Omega$, and set the unsteadiness parameter

$$\beta_0 = \nu^{\frac{1}{2}}\Omega^{-\frac{1}{2}}a^{-1}. \tag{1.2}$$

(Physically this may be interpreted as the ratio of the viscous length ($\nu^{\frac{1}{2}}\Omega^{-\frac{1}{2}}$) to a typical length ($a$).)

With these scalings, the continuity and Navier–Stokes equations may be written in the form

$$\operatorname{div} \mathbf{u} = 0, \tag{1.3}$$

$$\frac{1}{\beta_0^2}\frac{\partial \mathbf{u}}{\partial t} + K(\mathbf{u}.\nabla)\mathbf{u} = -\nabla p + \nabla^2 \mathbf{u} \tag{1.4}$$

where $\mathbf{u} = (u, v)$.

The channel walls are described by

$$\left.\begin{aligned} y &= hK^{-\frac{1}{3}}F(x,t) \quad \text{lower}, \\ y &= 1-hK^{-\frac{1}{3}}F(x,t) \quad \text{upper}, \end{aligned}\right\} \tag{1.5}$$

with
$$F(x \leqslant 0,t) = 0, \quad |hF(x,t)| \leqslant O(1). \tag{1.6}$$

The boundary conditions on these two walls are, first, the condition of no slip:

$$u(x, hK^{-\frac{1}{3}}F(x,t),t) = u(x, 1-hK^{-\frac{1}{3}}F(x,t),t) = 0, \tag{1.7}$$

and, second, that the normal velocity of the fluid on the walls must equal the wall velocity, i.e.

$$\left.\begin{aligned} v(x, hK^{-\frac{1}{3}}F(x,t),t) &= K^{-\frac{4}{3}}hF_t(x,t)/\beta_0^2, \\ v(x, 1-hK^{-\frac{1}{3}}F(x,t),t) &= -K^{-\frac{4}{3}}hF_t(x,t)/\beta_0^2. \end{aligned}\right\} \tag{1.8}$$

In addition the solution must join, far upstream, to the fully-developed (Poiseuille) motion:

$$u = U_0(y) = \tfrac{1}{2}(y-y^2), \quad v = 0, \quad p = p_D - x, \tag{1.9}$$

where p_D is an arbitrary constant. It should be noted that because of the nature of the problem there is a (time-dependent) discrepancy between the net flows far upstream and far downstream of the distortion, this discrepancy being related to the rate of change of area of the indented section. Consequently, in an experimental situation, in which the flow is driven by a prescribed pressure gradient, the condition of a steady flow far upstream might be difficult to achieve in practice. This situation is aggravated by the fact that the perturbation pressure is generally of higher order than the driving pressure (unless $|x| \gg 1$) and so very long channels would have to be used in any experimental situation. More quantitative details of this will be given in the discussion in §5.

Smith (1976*b*) considered the same basic problem. However, his discussion was limited to humps of slope (α) between $O(K^{-1})$ and $O(K^{-\frac{1}{3}})$ for symmetric flows, and between $O(K^{-1})$ and $O(K^{-\frac{3}{7}})$ for asymmetric flows, with $\beta_0 = O(\alpha K^{-\frac{1}{2}})$. Moreover, he assumed a small distortion height, i.e. $h \ll 1$, enabling him to obtain a perturbation solution, based on the upstream Poiseuille flow.

Here a study is made of the effects on the motion resulting from increasingly fast variations in the wall shape. We start in §2, by considering the case of moderate unsteadiness where $\beta_0 = K^{-\frac{1}{3}}\beta$, with $\beta = O(1)$. For this regime of the unsteadiness parameter, the problem (posed by Smith 1976*b*) is nonlinear and must be tackled numerically, although there is no appreciable upstream influence.

The reason for this nonlinearity is that with this order of β_0, and this size of hump, we find that in the boundary-layer approximation of the x-momentum equation, the time derivative term balances with the viscous diffusion and advection terms. The numerical results presented indicate, however, that as $\beta \to 0$ an analytic asymptotic description emerges. This description leads us on to consider next, in §3, 'fast' time variations defined by the order of magnitude $\beta_0 = O(K^{-\frac{1}{2}})$. For this case we find that the form of the solution is markedly different from the previous regime in a number of respects, including the presence of appreciable upstream influence, although asymptotic analysis is again possible. For this regime of β_0 it is found that the velocity induced by the motion of the wall balances with the oncoming Poiseuille flow in the streamwise momentum equation near the walls. The properties of the solution obtained in § 3 then lead us on further to study the order of magnitude $\beta_0 = O(K^{-\frac{2}{3}})$ ('very fast' time variations), for which yet another structure for the solution emerges, the velocity induced by the wall motion balancing with the on-coming Poiseuille flow in the core in the equations of motion. Further near the walls the effect of the distortion is dominant over the undisturbed flow up to distances $x = -(1/3\pi) \ln K + O(1)$ upstream of the wall distortions.

We find that with the appropriate limits of the unsteadiness parameter the results of § 3 reproduce the (limiting) results of § 2 and § 4, i.e. the asymptotic results obtained are commutative, as one might expect. Finally, the discussion of the results is presented in § 5.

2. Moderate unsteadiness ($\beta_0 = O(K^{-\frac{1}{3}})$)

We set $\beta_0 = K^{-\frac{1}{3}}\beta$, where $\beta = O(1)$ and we find, following Smith (1976*b*), that the flow consists of three zones: an inviscid rotational core motion (region 1 below), bounded by two viscous layers (region 2 below), adjoining the walls, which are identical for symmetrical wall motions.

Region 1. In the core zone where $0 < y < 1$, a perturbation to the Poiseuille flow is to be expected, the solution developing in the same form as of Smith (1976*b*), i.e.

$$\left.\begin{aligned} \psi &= \psi_0(y) + K^{-\frac{2}{3}}\psi_1(x,y,t) + \dots, \\ u &= U_0(y) + K^{-\frac{2}{3}}u_1(x,y,t) + \dots, \\ v &= K^{-\frac{2}{3}}v_1(x,y,t) + \dots \quad \text{and} \quad p = K^{\frac{1}{3}}p_1(x,y,t) + \dots, \end{aligned}\right\} \tag{2.1}$$

where $u = \psi_y$ and $v = -\psi_x$, and where $\psi_0(y)$ is the basic (Poiseuille) flow. Note that the driving pressure gradient is $O(1)$ and so the perturbation pressure dominates in the pressure expansion.

With the expansions of (2.1), the governing equations (1.4) yield, for $\beta_0 = O(K^{-\frac{1}{3}})$

$$U_0 \nabla^2 v_1 = v_1 U_{0yy}, \quad v_{1y} + u_{1x} = 0, \tag{2.2}$$

with the two constraints:

$$\left.\begin{aligned} &v_1(x, \tfrac{1}{2}) = 0 \quad \text{(symmetry condition)}, \\ &v_1(x, 0) = -2\frac{\partial P_0}{\partial x}(x,t) \quad \text{(defined below)}. \end{aligned}\right\} \tag{2.3}$$

This differential system is similar to that obtained by Smith (1976*b*) for flow in symmetrical, steady channels of distortions of slope $O(K^{-\frac{1}{3}})$, and so for moderate unsteadiness time dependence appears only parametrically [through the pressure gradient in (2.3)]. In the core, as noted by Smith (1976*b*) the system described above may be solved by extending the analysis of Tillet (1968) for the problem of the liquid jet emerging from a channel.

Because the condition of no slip on the walls has been relaxed in (2.2)–(2.3), a viscous wall layer is required, from which the pressure gradient $\partial P_0/\partial x$ is determined:

Region 2. In the lower viscous wall layer, where $y = K^{-\frac{1}{3}}(z + hF)$ and where $z = O(1)$, the solution may be expanded in the form (again following Smith 1976*b*)

$$\psi = K^{-\frac{2}{3}}\Psi_0(x,z,t) + \dots, \quad p = K^{\frac{1}{3}}P_0(x,t) + \dots. \tag{2.4}$$

Using (1.4) again, the equation for Ψ_0 is the unsteady boundary-layer equation, i.e.

$$\frac{1}{\beta^2}[\Psi_{0zt} - hF_t\Psi_{0zz}] + \Psi_{0z}\Psi_{0zx} - \Psi_{0x}\Psi_{0zz} = -\frac{\partial P_0}{\partial x} + \Psi_{0zzz} \tag{2.5}$$

with $\quad P_0 \equiv P_0(x,t) \quad$ and $\quad \Psi_{0x}(z=0) = -hF_t/\beta^2, \quad \Psi_{0z}(z=0) = 0, \quad$ (2.6)

and, as $z \to \infty$,

$$\Psi_0 \to 2P_0 + \tfrac{1}{4}(z+hF)^2. \tag{2.7}$$

We now consider the numerical solution of this system.

When there is a discontinuous change in wall shape at $x = 0$, the flow adjusts in a singular fashion to the distortion, the effects of the wall growing inside a sublayer of thickness $O(x^{\frac{1}{3}})$ for $0 \leqslant x \ll 1$. In fact inspection of the unsteady boundary-layer equation (2.5) reveals that the solution may be expected to develop in the form:

$$\left.\begin{aligned} \Psi_0 &= \tfrac{1}{4}z^2 + \xi^4 G_1(\eta, t) + O(\xi^5) \\ \text{where} \qquad \eta &= z/\xi = O(1), \quad \xi = x^{\frac{1}{3}}. \end{aligned}\right\} \tag{2.8}$$

Consequently, in order that the numerical scheme should be accurate near $x = 0$, for discontinuous wall shapes, the stream function must be expressed as follows:

$$\Psi_0 = \xi^2 H(\xi, \eta, t) \tag{2.9}$$

whilst the pressure is written in the form

$$P_0 = \xi^4 Q(\xi, t). \tag{2.10}$$

Note that for smooth wall shapes it is possible to work with the original physical variables – Ψ_0, P_0, x and z – but the general numerical method to be described would otherwise remain the same.

When we write

$$c = H_\eta, \quad e = c_\eta, \tag{2.11}$$

then in the new co-ordinate system, (2.5) becomes

$$\frac{1}{\beta^2}[\xi^2 c_t - h\xi F_t e] + \tfrac{1}{3}c^2 + \frac{\xi}{3}cc_\xi - \tfrac{2}{3}eH - \frac{\xi}{3}eH_\xi = -\left(\frac{4\xi^2}{3}Q + \frac{\xi^3}{3}Q_\xi\right) + e_\eta. \tag{2.12}$$

The three first-order differential equations represented by (2.11) and (2.12) were approximated by three finite difference equations. With step lengths $\Delta\xi$, $\Delta\eta$ and Δt, the (second-order accurate) differencing of (2.11) was centred at points $(\xi_i, \eta_j - \frac{1}{2}\Delta\eta, t_k)$ whilst (2.12) was differenced (and averaged) about $(\xi_i - \frac{1}{2}\Delta\xi, \eta_j - \frac{1}{2}\Delta\eta, t_k - \frac{1}{2}\Delta t)$, where (ξ_i, η_j, t_k) are the (ith, jth, kth) points in the (ξ, η, t) directions. A Newton iteration scheme was employed to deal with the nonlinearity of the equations, and the resulting matrix equation for the increments $\delta H(\xi_i, \eta_j, t_k)$, $\delta c(\xi_i, \eta_j, t_k)$ and $\delta e(\xi_i, \eta_i, t_k)$, $j = 1$, N was then solved by Gaussian elimination, the diagonal nature of the 'left-hand side' of the equation being fully exploited in a manner explained by Smith (1974). The solution was obtained by marching first in the ξ and then in the t direction, because of the parabolic nature of the boundary layer equations. In the calculations, step lengths of $\Delta\eta = 0{\cdot}25$ and $\Delta\xi = 0{\cdot}0625$ were found adequate, with 'infinity' in the η direction being taken at $\eta = 10$. Since the solutions were started from the unperturbed state, the step lengths in time were generally started at 0·001 (or even smaller, if necessary), and

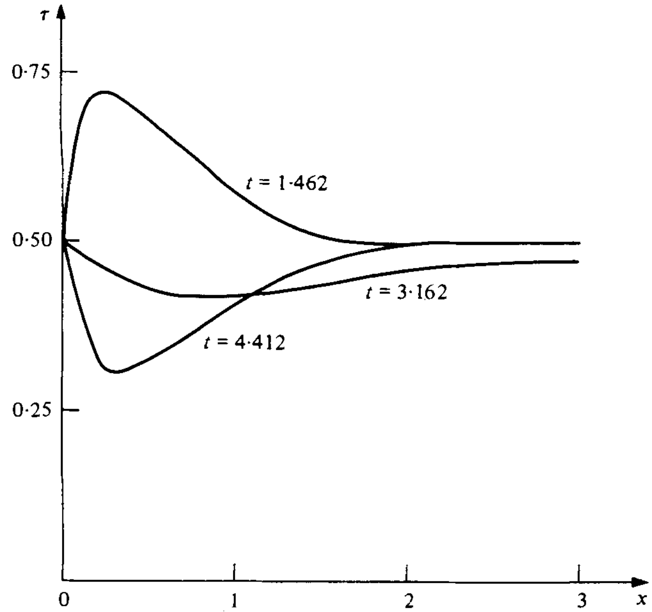

FIGURE 2. Wall shear distributions for $\beta = 1$, $h = 1$ (nonlinear solution).

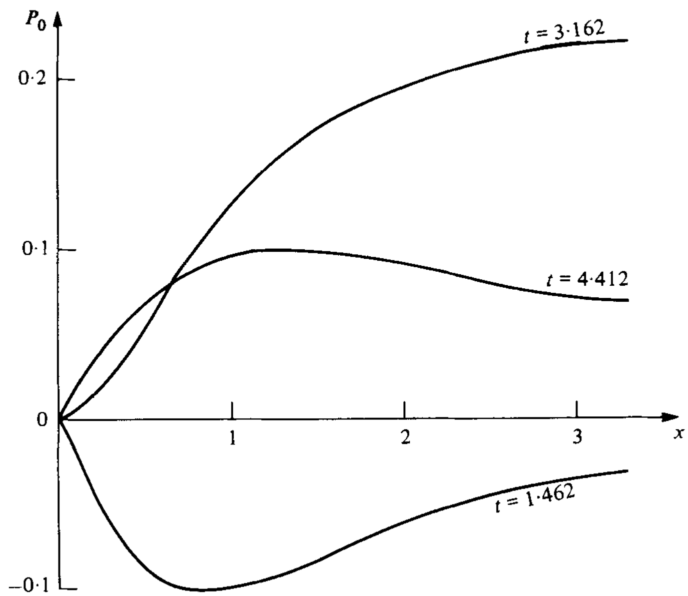

FIGURE 3. Excess wall pressure distributions for $\beta = 1$, $h = 1$ (nonlinear solution).

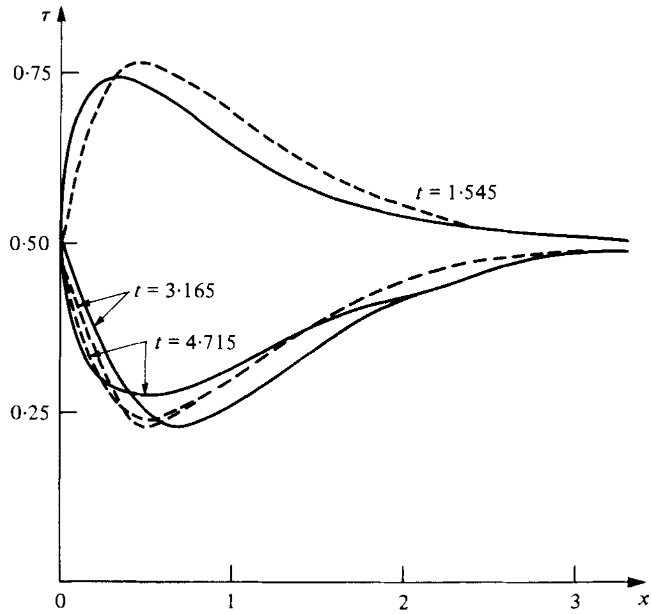

FIGURE 4. Wall shear distributions for $\beta = 0{\cdot}5$, $h = 1$ (dashed lines denote asymptotic solutions, solid lines nonlinear solutions).

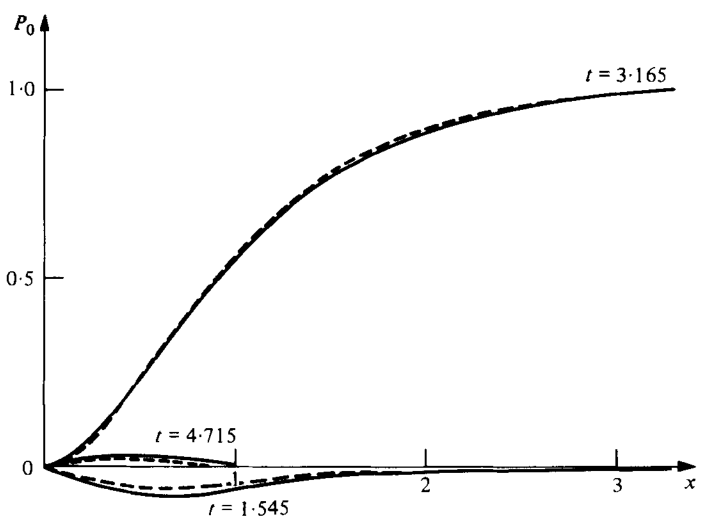

FIGURE 5. Excess wall pressure distributions for $\beta = 0{\cdot}5$, $h = 1$ (dashed lines denote asymptotic solutions, solid lines nonlinear solutions).

gradually increased to about 0·05 as the calculation progressed. Usually just four or five iterations were required for convergence (defined when the maximum change in any of the calculated flow quantities was 10^{-8}).

Some of the results of sets of calculations are presented in figures 2–6, which show wall perturbation pressure and wall shear ($\Psi_{0zz}(x, 0, t)$) distributions for distortions of the form

$$F(x,t) = 2H(t)\,H(x)\,x\,e^{-2x}\sin t \tag{2.13}$$

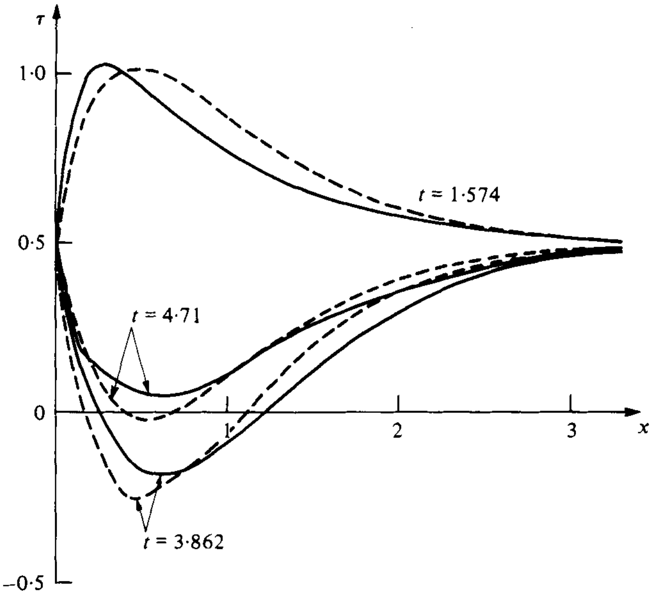

FIGURE 6. Wall shear distributions for $\beta = 0{\cdot}5$, $h = 2$ (dashed lines denote asymptotic solutions, solid lines nonlinear solutions).

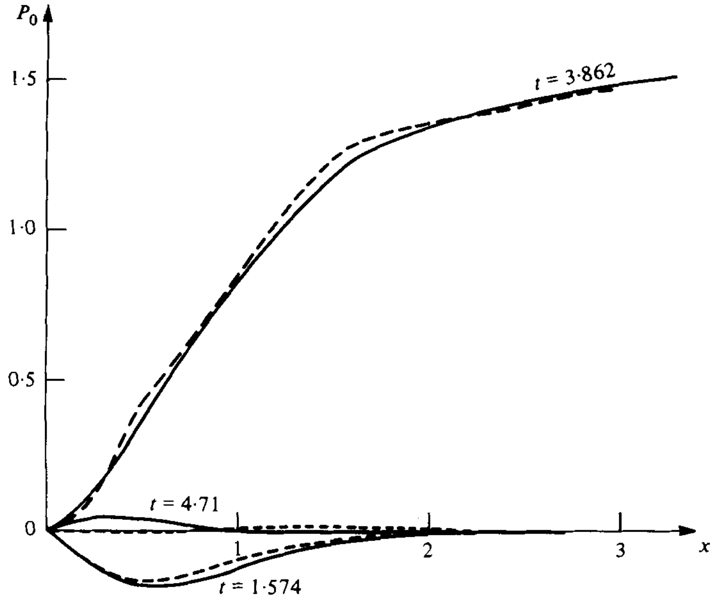

FIGURE 7. Excess wall pressure distributions for $\beta = 0{\cdot}5$, $h = 2$ (dashed lines denote asymptotic solutions, solid lines nonlinear solutions).

where $H(t)$ is the Heaviside function. This form corresponds to a wall, initially at rest and unperturbed, which at $t = 0$ suddenly begins to move sinusoidally. Figures 2 and 3 are for the case $h = 1$, $\beta = 1$, at three particular instants in time. As the hump rises, the shear increases and the excess wall pressure falls over the hump (the reverse occurs when the hump is falling). As $x \to \infty$, the shear returns to its Poiseuille value of $\frac{1}{2}$, whilst the pressure appears to asymptote to a constant value. Interestingly enough, these and all the results obtained indicated that the solution settled down to a periodic form very quickly, in spite of the impulsive start to the wall motion. Figures 4 and 5 are for $h = 1$, $\beta = \frac{1}{2}$ and the results show similar trends to those of the previous set. The most noticeable difference is the change in the order of the pressure for $t \approx 3{\cdot}16$ in the two cases, the pressure this time asymptoting to a value about four times that of the previous example. The third set, shown in figures 6 and 7, are for $h = 2$, $\beta = \frac{1}{2}$, and we see that as the hump is falling a region of flow reversal occurs owing to the large, adverse pressure gradient encountered. Although the numerical scheme is strictly invalid in such regions, this type of phenomenon has been encountered by a number of authors, for instance Stewartson & Williams (1969). Because the negative velocities in the example were small, and the region in which such reversals occurred was small, the numerical scheme continued to converge. In spite of these regions of flow reversal, again the pressures appear to asymptote to particular constant values downstream.

We now consider, briefly, the asymptotic behaviour downstream, i.e. as $x \to +\infty$. We shall consider, following our numerical work, distortions that decay exponentially downstream. Then the boundary conditions (2.6) become, as $x \to +\infty$:

$$\Psi_0(z \to \infty) \to 2P_0 + \tfrac{1}{4}z^2 + \text{exponentially small terms}; \tag{2.14}$$

$$\Psi_0(z = 0) = -\frac{hG_t}{\beta^2} = -\int_0^\infty \frac{hF_t}{\beta^2}\, dx. \tag{2.15}$$

The solution of (2.5) as $x \to +\infty$, together with (2.14) and (2.15) appears to be

$$\Psi_0 \to -\frac{hG_t}{\beta^2} + \tfrac{1}{4}z^2, \tag{2.16a}$$

$$P_0 \to -\frac{hG_t}{2\beta^2}. \tag{2.16b}$$

This then shows clearly the pressure asymptoting as $x \to +\infty$, as noted in the numerical results. Although an exponential decay was assumed, for algebraically decaying distortion heights (provided the perturbation height decays faster than $1/x$ as $x \to +\infty$) then the asymptotic expressions for ψ_0 and P_0 will be given by (2.16) also.

$\beta \to \infty$ results in a quasi-steady type of solution to first order, the steady solution being that of Smith (1976*a*).

As $\beta \to 0$ the numerical results suggest that the pressure behaves as β^{-2}. This in particular suggests that (for x, z, t of $O(1)$) as $\beta \to 0$ we may expect asymptotic expansions of the form

$$\left.\begin{aligned} \Psi_0 &= \frac{\Psi_{00}}{\beta^2} + \Psi_{01} + \beta\Psi_{02} + \beta^2\Psi_{03} + O(\beta^3),\\ P_0 &= \frac{p_{00}}{\beta^2} + p_{01} + \beta p_{02} + \beta^2 p_{03} + O(\beta^3). \end{aligned}\right\} \tag{2.17}$$

The $O(\beta^{-2})$ terms arise essentially from the motion of the wall whilst the equation of motion (2.5) shows that there are to be no $O(\beta^{-1})$ terms. Substituting these expansions into the governing equation (2.5), and equating like powers of β, we find first the following simple uniformly valid solution:

$$\Psi_{00} = -hG_t, \quad p_{00} = -\tfrac{1}{2}hG_t \quad \text{where} \quad G(x,t) = \int_0^x F(x,t)\,dx \tag{2.18}$$

which satisfies the boundary conditions both at the wall and at $z = \infty$. However, when considering Ψ_{01} we find it is not possible to satisfy all the boundary conditions. Relaxing the condition of no slip at $z = 0$, we find in fact

$$\Psi_{01} = \tfrac{1}{2}zhF + \tfrac{1}{4}z^2, \quad p_{01} = \tfrac{1}{8}h^2F^2. \tag{2.19}$$

Consequently a further inner (Stokes) layer of thickness $O(K^{-\frac{1}{3}}\beta)$ is required in order that the no-slip boundary condition may be satisfied. In this layer, the stream function and z are rescaled as follows

$$\left(\Psi_0 + \frac{hG_t}{\beta^2}\right) = \beta\hat{\Psi} = \beta(\hat{\Psi}_0 + \beta\hat{\Psi}_1 + \beta^2\hat{\Psi}_2 + \ldots), \quad z = \beta\hat{z} \tag{2.20}$$

where $\hat{\Psi}$ and $\hat{z}$ are both $O(1)$ quantities in this inner layer. Then, from substituting (2.20) into (2.5), $\hat{\Psi}_0$ is governed by the linear (Stokes) equation

$$\hat{\Psi}_{0\hat{z}\hat{z}\hat{z}} - \hat{\Psi}_{0\hat{z}t} = \frac{-hF_t}{2}. \tag{2.21}$$

As an example, if the hump oscillates sinusoidally, then $F(x,t)$ may be expressed in the form

$$F(x,t) = f(x)\,e^{it} + \text{c.c.} \tag{2.22}$$

where 'c.c.' denotes a complex conjugate, and then the solution of (2.21) is

$$\hat{\Psi}_0 = \frac{hf}{2}\exp(it)\left\{\frac{1-i}{\sqrt{2}}\left[\exp\left(-(1+i)\,\hat{z}/\sqrt{2}\right) - 1\right] + \hat{z}\right\} + \text{c.c.} \tag{2.23}$$

The process may be continued to higher orders of β, and gives

$$\Psi_{02} = 2p_{02} = \frac{-hf}{2\sqrt{2}}(1-i)\exp(it) + \text{c.c.}, \quad \hat{\Psi}_1 = \tfrac{1}{4}\hat{z}^2 \tag{2.24}$$

($\hat{\Psi}_1$ arising directly from the basic Poiseuille flow).

At $O(\beta^0)$ in (2.5) the governing equation is

$$\Psi_{03zt} = 0.$$

Now we set

$$\Psi_{03} = \Psi_{03}^{(s)}(x,z) + \Psi_{03}^{(u)}(x,t), \tag{2.25}$$

i.e. Ψ_{03} has been split into a steady and an unsteady component. $\Psi_{03}^{(s)}$ and $\Psi_{03}^{(u)}$ will be considered later, once $\hat{\Psi}_2(x,\hat{z},t)$ has been determined, from

$$\hat{\Psi}_{2\hat{z}t} + \hat{\Psi}_{0\hat{z}}\hat{\Psi}_{0\hat{z}x} - \hat{\Psi}_{0x}\hat{\Psi}_{0\hat{z}\hat{z}} = -p_{01x} + \hat{\Psi}_{2\hat{z}\hat{z}\hat{z}} \tag{2.26}$$

with the following boundary conditions on $\hat{z} = 0$:

$$\hat{\Psi}_2(x,0,t) = \hat{\Psi}_{2\hat{z}}(x,0,t) = 0. \tag{2.27}$$

The boundary conditions as $\hat{z} \to \infty$ will be discussed later. We also find it convenient to split $\hat{\Psi}_2$ and p_{03} into two components – the one steady, the other (periodic) time dependent, i.e.

$$\left.\begin{aligned}\hat{\Psi}_2(x,z,t) &= \hat{\Psi}_2^{(s)}(x,\hat{z}) + \hat{\Psi}_2^{(u)}(x,\hat{z},t),\\ p_{03}(x,t) &= p_{03}^{(s)}(x) + p_{03}^{(u)}(x,t).\end{aligned}\right\} \tag{2.28}$$

Then it is found possible to satisfy boundary conditions (2.27) for $\hat{\Psi}_2^{(u)}$, together with the condition

$$\hat{\Psi}_{2\hat{z}}^{(u)}(x,\hat{z},t) \to 0 \quad \text{as} \quad \hat{z} \to \infty, \tag{2.29}$$

implying

$$\Psi_{03}^{(u)}(x,t) \equiv p_{03}^{(u)}(x,t) \equiv 0. \tag{2.30}$$

Specifically, we find, from (2.26)

$$\hat{\Psi}_2^{(u)} = \tfrac{1}{8}h^2 f f_x\{(1+i)[\exp(-(1+i)\hat{z})-1] + 2i\hat{z}\exp[-(1+i)\hat{z}/\sqrt{2}]\}\exp(2it) + \text{c.c.} \tag{2.31}$$

Consider now $\hat{\Psi}_2^{(s)}$: Writing

$$\hat{\Psi}_2^{(s)} = X_2^{(s)} + \text{c.c.}, \quad \hat{\Psi}_0 = X_0 \exp(it) + \text{c.c.} \tag{2.32}$$

where, from (2.23)

$$X_0 = \frac{hf}{2}\left\{\frac{1-i}{\sqrt{2}}[\exp(-(1+i)\hat{z}/\sqrt{2})-1] + \hat{z}\right\}. \tag{2.33}$$

Then the governing equation for $X_2^{(s)}$ is

$$X_{2\hat{z}\hat{z}\hat{z}}^{(s)} = -\tfrac{1}{4}h^2 f\bar{f}_x - \bar{X}_{0x}X_{0\hat{z}\hat{z}} + \bar{X}_{0\hat{z}}X_{0\hat{z}x} \tag{2.34}$$

(a bar denoting a complex conjugate).

Although conditions (2.27) may be satisfied, it is not possible to solve (2.34) subject to a condition of the form (2.29), i.e. the inner boundary layer produces a steady outer slip which must be used as an inner condition in the solution of $\Psi_{03}^{(s)}(x,z)$. In fact $X_2^{(s)}$ is given by

$$\begin{aligned}X_2^{(s)} = \frac{h^2}{4}f\bar{f}_x\bigg\{&\frac{\hat{z}}{2}(i-3) + \frac{1}{2\sqrt{2}}(13+3i) - \frac{(1-i)}{2\sqrt{2}}\exp(-\sqrt{2}\hat{z}) - \sqrt{2}\exp[-(1+i)\hat{z}/\sqrt{2}]\\ &+\frac{1}{\sqrt{2}}(-1+i)\exp[-(1-i)\hat{z}/\sqrt{2}] - i\hat{z}\exp[-(1+i)\hat{z}/\sqrt{2}]\\ &-\frac{3}{\sqrt{2}}(1+i)\exp[-(1+i)\hat{z}/\sqrt{2}]\bigg\}.\end{aligned} \tag{2.35}$$

This produces an outer slip of

$$X_{2\hat{z}}^{(s)}(x,\hat{z}) \to V(x) = \frac{h^2 f\bar{f}_x}{8}(i-3) \quad \text{as} \quad \hat{z} \to \infty \tag{2.36}$$

to give the inner boundary condition for $\Psi_{03}^{(s)}(x,z)$. We shall not, for the sake of brevity, consider the governing equation for Ψ_{04} (which will be seen to be unnecessary for the present purposes) except to note that this equation (which is obtained from considering the $O(\beta)$ terms in (2.5)) is the first in which there is a non-trivial interaction between the Poiseuille flow and the velocity induced by the wall motion.

Considering now the $O(\beta^2)$ terms in (2.5) we find

$$\Psi_{05zt} + [\tfrac{1}{2}hF + \tfrac{1}{2}z]\Psi_{03zx} + \tfrac{1}{2}hF_x\Psi_{03z} - \tfrac{1}{2}zhF_x\Psi_{03zz} - \tfrac{1}{2}\Psi_{03x} = -p_{03x} + \Psi_{03zzz}. \tag{2.37}$$

However, we already know that

$$\Psi_{03} = \Psi_{03}^{(s)}(x,z), \quad p_{03} = p_{03}^{(s)}(x) \text{ only,} \tag{2.38}$$

and so equating just the steady terms in (2.37) gives

$$\tfrac{1}{2}z\Psi_{03zx}^{(s)} - \tfrac{1}{2}\Psi_{03x}^{(s)} = -p_{03x}^{(s)} + \Psi_{03zzz}^{(s)}. \tag{2.39}$$

Differentiating with respect to z, and applying the Fourier transform with respect to x, with

$$\Psi_{03}^{*} = \int_{-\infty}^{\infty} \Psi_{03}^{(s)} \exp(-i\omega x)\, dx, \tag{2.40}$$

yields

$$\Psi_{03zz}^{*} = A(\omega)\, \mathrm{Ai}\left[z\left(\frac{i\omega}{2}\right)^{\frac{1}{3}}\right] \tag{2.41}$$

and so

$$\Psi_{03}^{*} = U^{*}\left\{-3\left(\frac{i\omega}{2}\right)^{\frac{1}{3}} \int_0^z \int_0^z \mathrm{Ai}\left[z\left(\frac{i\omega}{2}\right)^{\frac{1}{3}}\right] dz\, dz + z\right\} \tag{2.42}$$

where $U^{*} = (V^{*} + \bar{V}^{*})$ is the Fourier transform of the inner slip, $V(x)$ given by (2.34). The transform of the pressure term $P_{03}^{(s)}$ is

$$p_{03}^{*} = \tfrac{1}{2}U^{*}\left(\frac{i\omega}{18}\right)^{-\frac{1}{3}} \Big/ \Gamma(\tfrac{1}{3}). \tag{2.43}$$

A comparison between the pressure and shear distribution using the above asymptotic theory for $\beta \to 0$ and the numerical results discussed earlier is shown in figures 4–7, the asymptotic theory results denoted by dashed lines. This reveals that even for $\beta = \frac{1}{2}$, the numerical results (particularly the pressure) discussed previously in this section are described remarkably well by the asymptotic theory. Note also that the results of this $\beta \to 0$ analysis as $x \to \infty$ reproduce the asymptotic forms of the full nonlinear system.

This $\beta \to 0$ theory leads us to inspect the next regime of β_0, namely $\beta = O(K^{-\frac{1}{2}})$ when the form of the core solution changes, with time derivatives first appearing in the governing equation in the core.

3. Fast time variations ($\beta_0 = O(K^{-\frac{1}{2}})$)

Let us write $\beta_0 = K^{-\frac{1}{2}}\beta_1$, where β_1 is $O(1)$. In the core zone, guided by the results from the previous section for moderate unsteadiness, we again expect the effect of the hump to be a small perturbation to the upstream Poiseuille flow $\psi_0(y)$, but this time expand the solution as follows.

Region 1.

$$\left.\begin{aligned} \psi &= \psi_0(y) + K^{-\frac{1}{3}}\psi_1(x,y,t) + \dots, \\ p &= K^{\frac{2}{3}}p_1(s,y,t) + \dots \end{aligned}\right\} \tag{3.1}$$

where ψ_1 is described by

$$\frac{1}{\beta_1^2}\nabla^2\psi_{1t} - \psi_{1x}\psi_{0yyy} + \psi_{0y}\nabla^2\psi_{1x} = 0$$

with

$$\psi_1(x,0) = -hG_t/\beta_1^2, \quad \psi_{1x}(x,\tfrac{1}{2}) = 0. \tag{3.2}$$

The solution appears difficult in general – the equation being essentially the Rayleigh equation, with additional (time derivative) terms. However, the solution may be accomplished in two extremes. First, in the limit $\beta_1 \to \infty$, the equation in the core reduces to a quasi-steady form, essentially the same as that of (2.2), and, as noted earlier, has been discussed by Smith (1976*b*) (although in the wall layers the flow will be truly unsteady, and will be seen to match the results in § 2 as $\beta \to 0$). Second, taking the other limit, as $\beta_1 \to 0$, the equation reduces to the form

$$\frac{\partial}{\partial t}(\nabla^2 \psi_1) = 0. \tag{3.3}$$

Taking Fourier transforms in the x direction and using asterisks to denote transformed variables:

$$\psi_1^* = \int_{-\infty}^{\infty} \psi_1(x, y, t)\, e^{-i\omega x}\, dx \tag{3.4}$$

then $\psi_1^* = A(\omega) \sinh \omega(y - \frac{1}{2})$.

Using the boundary conditions gives

$$\psi_1^* = \frac{hG_t^*(\omega)}{\beta_1^2} \sinh \omega(y - \tfrac{1}{2}) \operatorname{cosech} \tfrac{1}{2}\omega \tag{3.5}$$

so that

$$\psi_1 = \frac{1}{2\pi} \int_{-\infty}^{\infty} \frac{hG_t^*(\omega) \sinh \omega(y - \frac{1}{2})\, e^{ixx}}{\beta_1^2 \sinh \frac{1}{2}\omega}\, d\omega. \tag{3.6}$$

In particular the slip at $y = 0$, for $x < 0$, is (using contour integration in the lower half of the ω plane)

$$u_1(x, t) = \psi_{1y}(x, 0, t) = \frac{1}{\beta_1^2} \sum_{m=1}^{\infty} 4m\pi\, hG_t^*(-2im\pi)\, e^{2m\pi x}. \tag{3.7a}$$

Whilst for $x > 0$ we find the slip on $y = 0$ is

$$u_1(x, t) = \frac{1}{\beta_1^2} \sum_{m=1}^{\infty} 4m\pi\, hG_t^*(2im\pi)\, e^{-2m\pi x}. \tag{3.7b}$$

Although the above is for $\beta_1 \to 0$, the $\beta_1 = O(1)$ case would also produce a slip of this kind. Note that the solution now has upstream influence, and so we require an inner (boundary-layer type) solution upstream of the hump, as well as over the hump itself.

Region 2. Returning to the case when β_1 is $O(1)$, we scale variables in the boundary layer in the following manner:

$$y = K^{-\frac{1}{3}}(hF + z), \tag{3.8}$$

$$\psi + \frac{hG_t}{\beta_1^2} K^{-\frac{1}{3}} = K^{-\frac{2}{3}} \Psi, \tag{3.9}$$

$$p = K^{\frac{2}{3}} P(x, t), \tag{3.10}$$

with

$$\frac{\partial P}{\partial x} = \frac{\partial p_1}{\partial x}(x, 0, t) = \frac{-1}{\beta_1^2} \left\{ \frac{\partial u_1}{\partial t} + \frac{hF_t}{2} \right\}, \tag{3.11}$$

where z, Ψ, P are $O(1)$ quantities inside this boundary layer, and u_1 is the slip produced by the outer solution (given by (3.7) for the case $\beta_1 \to 0$). Note that upstream of the hump ($x < 0$),

$$F \equiv G \equiv 0. \tag{3.12}$$

The results of the previous section suggest that Ψ must be expanded as follows:

$$\Psi = \Psi_0 + K^{-\frac{1}{6}}\Psi_1 + O(K^{-\frac{1}{3}}). \tag{3.13}$$

Using (1.4), Ψ_0 is found to be governed by

$$\frac{1}{\beta_1^2}\Psi_{0zt} = -\frac{\partial P}{\partial x} \tag{3.14}$$

so that

$$\Psi_0 = \tfrac{1}{4}z^2 + z\left\{u_1 + \frac{hF}{2}\right\}. \tag{3.15}$$

This implies that the inner condition of no slip is not satisfied, and so, rescaling again inside:

Region 3. We introduce a further inner (Stokes) layer by scaling

$$\Psi = K^{-\frac{1}{6}}\hat{\Psi}, \quad z = K^{-\frac{1}{6}}\hat{z} \tag{3.16}$$

(the pressure scaling is unchanged), where $\hat{\Psi}$ is expanded in the following manner

$$\hat{\Psi} = \hat{\Psi}_0 + K^{-\frac{1}{6}}\hat{\Psi}_1 + \dots. \tag{3.17}$$

(This is suggested, again, by the previous section.) Then from (1.4) $\hat{\Psi}_0$ is to be determined from the linear Stokes layer equation:

$$\frac{1}{\beta_1^2}\hat{\Psi}_{0\hat{z}t} = \frac{1}{\beta_1^2}\frac{\partial u_1}{\partial t} + \frac{hF_t}{2} + \Psi_{0\hat{z}\hat{z}\hat{z}} \tag{3.18}$$

with boundary conditions:

$$\hat{\Psi}_0(x,0,t) = \hat{\Psi}_{0\hat{z}}(x,0,t) = 0. \tag{3.19}$$

To match with $\hat{\Psi}_0$ the solution above, we must have

$$\Psi_{0\hat{z}}(x,\hat{z},t) \to u_1(x,t) + \tfrac{1}{2}hF(x,t) \quad \text{as} \quad \hat{z} \to \infty. \tag{3.20}$$

If we restrict our discussion to oscillatory humps (of the form (2.22)), then we may write

$$\tfrac{1}{2}hF(x,t) + u_1(x,t) = v_1(x)\,e^{it} + \text{c.c.} \tag{3.21}$$

and using (3.18)–(3.20) gives

$$\hat{\Psi}_0 = v_1\left\{\hat{z} + \frac{1-i}{\sqrt{2}}\beta_1\left[\exp\left(-(1+i)\,\hat{z}/\sqrt{2}\beta_1\right) - 1\right]\right\} + \text{c.c.} \tag{3.22}$$

Note that as $\beta_1 \to \infty$, the fast variation solution matches with the previous case of moderate unsteadiness, $\beta_0 = O(K^{-\frac{1}{3}})$. For $\beta_0 = O(K^{-\frac{1}{2}})$, we see sizeable upstream influence appearing in the solution and growing. The region where the flow begins to pulsate appreciably moves upstream, away from the hump as β_1 becomes smaller, although the behaviour of the path of this region depends on detailed knowledge of the core solution (i.e. the solution of (3.2)).

We next go on to consider the very fast variation case $\beta_0 = O(K^{-\frac{2}{3}})$ when the character of the core solution changes once again, with the effect of the disturbance of the wall being of the same order as the basic flow in the core.

4. Very fast time variations ($\beta_0 = O(K^{-\frac{2}{3}})$)

This time set $\beta_0 = K^{-\frac{2}{3}}\beta_2$, with $\beta_2 = O(1)$. From the results of the previous regime of β_0 (in particular as $\beta_1 \to 0$) we can expect the solution in the core zone to develop in the form

$$\left.\begin{aligned} \psi &= \psi_0(x,y,t)+\ldots, \\ P &= K^{\frac{4}{3}}P_1(x,y,t)+\ldots \end{aligned}\right\} \tag{4.1}$$

and so now the effect of the hump is of the same order as the Poiseuille flow in the core.

From (1.4), the equation for ψ_0 is found to be

$$\frac{\partial(\nabla^2\psi_0)}{\partial t} = 0 \tag{4.2}$$

with the following boundary conditions:

$$\psi_0(x,0,t) = hG_t/\beta_2^2, \quad \psi_{0x}(x,\tfrac{1}{2},t) = 0.$$

If ψ_0 is split into two components, one steady, the other unsteady:

$$\psi_0 = \psi_0^{(u)}(x,y,t)+\psi_0^{(s)}(x,y), \tag{4.3}$$

then in order to satisfy the upstream boundary conditions $\psi_0^{(s)}$ must be the solution for Poiseuille flow, whilst $\psi_0^{(u)}$ may be identified directly with ψ_1 described by (3.6). $\psi_0^{(u)}$ will produce a slip on the (lower) channel wall, described by

$$u_1(x,t) = \psi_{0y}^{(u)}(x,0,t) \tag{4.4}$$

(with a similar expression for the upper channel wall) and so again a boundary layer of thickness $O(K^{-\frac{1}{3}})$ is required near $y = 0$, in which variables are scaled as follows:

$$\left.\begin{aligned} \psi+\frac{hG_t}{\beta_2^2} &= K^{-\frac{1}{3}}\Psi, \\ p &= K^{\frac{4}{3}}P(x,t), \end{aligned}\right\} \tag{4.5}$$

and

$$y = K^{-\frac{1}{3}}(z+hF). \tag{4.6}$$

If Ψ and P are expanded in the form:

$$\left.\begin{aligned} \Psi &= \Psi_0+K^{-\frac{1}{3}}\Psi_1+\ldots, \\ P &= P_0+K^{-\frac{1}{3}}P_1+\ldots, \end{aligned}\right\} \tag{4.7}$$

then, from the Navier–Stokes equations, (1.4), Ψ_0 is to be found from

$$\Psi_{0zt} = -\frac{\partial P_0}{\partial x}, \tag{4.8}$$

and so to match with the core solution, we must have that

$$\Psi_0 = u_1 z. \tag{4.9}$$

Again, a further boundary (Stokes) layer is needed in order to reduce the slip to zero at the wall, this time of thickness $O(K^{-\frac{2}{3}})$. Now $O(1)$ variables $\hat{\Psi}$, $\hat{z}$ are introduced as follows:

$$\left.\begin{aligned} z &= K^{-\frac{1}{3}}\hat{z}, \\ \Psi+\frac{hG_t}{\beta_2^2} &= K^{-\frac{2}{3}}\hat{\Psi} = K^{-\frac{2}{3}}[\hat{\Psi}_0+O(K^{-\frac{1}{3}})]. \end{aligned}\right\} \tag{4.10}$$

By (1.4), Ψ_0 is the solution to

$$\frac{1}{\beta_2^2}\hat{\Psi}_{0\hat{z}t} = \frac{1}{\beta_2^2}\frac{\partial u_1}{\partial t} + \hat{\Psi}_{0\hat{z}\hat{z}\hat{z}}. \tag{4.11}$$

For oscillatory humps, i.e. those described by (2.22), we may write, for $x < 0$:

$$\Psi_0 = iv_1(x)\exp(it)\left\{\hat{z} + \frac{\beta_2(1-i)}{\sqrt{2}}\left[\exp\left(-(1+i)\,\hat{z}/\sqrt{2}\,\beta_2\right) - 1\right]\right\} + \text{c.c.} \tag{4.12}$$

where
$$v_1(x) = \sum_{m=1}^{\infty}\frac{4ihm\pi}{\beta_2^2}\,g^*(-2im\pi)\exp(2m\pi x)$$

with
$$g(x) = \int_0^x f(x)\,dx. \tag{4.13}$$

As a further example, to illustrate how the analysis can treat non-periodic movements, consider the case of initially flat walls, which suddenly, at $t = 0$, start to grow humps (a constriction) in a linear manner, i.e.

$$F(x,t) = tH(t)f(x), \tag{4.14}$$

where $H(t)$ is the Heaviside function, and where $|f(x)| \leqslant O(1)$. Note that although this is not an oscillatory motion, there will still be a single timescale associated with this motion, namely the time for the (dimensional) height of the distortion to rise $O(aK^{-\frac{1}{3}})$ (where a is the undistorted channel width). Obviously as $t \to \infty$ we expect the solution to break down, because of the condition $|hF(x,t)| \leqslant O(1)$ being violated, none the less we find

$$u_1(x,t) = H(t)\,tv_1(x) \tag{4.15}$$

where $v_1(x)$ is given by (4.13). Ψ_0 then is described by (4.9) and (4.11) becomes

$$\frac{1}{\beta_2^2}\hat{\Psi}_{0\hat{z}t} = \frac{H(t)\,v_1(x)}{\beta_2^2} + \hat{\Psi}_{0\hat{z}\hat{z}\hat{z}}. \tag{4.16}$$

Using Laplace transforms we find

$$\hat{\Psi}_0 = v_1(x)\left\{\hat{z}t - \frac{4t^{\frac{3}{2}}\beta_2}{3\sqrt{\pi}} + 8t^{\frac{3}{2}}\beta_2\, i^3\,\mathrm{erfc}\left(\frac{\hat{z}}{2\beta_2\sqrt{t}}\right)\right\} \tag{4.17}$$

where
$$i^n\,\mathrm{erfc}\,\eta = \int_\eta^\infty i^{n-1}\,\mathrm{erfc}\,\eta\,d\eta, \quad n = 1, 2, 3, \ldots \tag{4.18}$$

and $i^0\,\mathrm{erfc}\,\eta = \mathrm{erfc}\,\eta$.

Returning now to the general problem, consider the region far upstream where, in the core, the Poiseuille flow and the disturbance component of the flow are no longer of the same order. In other words, we are considering how far upstream the effect of the unsteady wall permeates.

From (4.13), we see that as $x \to -\infty$:

$$v_1(x) \sim \frac{4i\pi h}{\beta_2^2}\,g^*(-2i\pi)\,e^{2\pi x}. \tag{4.19}$$

The first change to the solution will occur when $v_1(x) = O(K^{-\frac{1}{3}})$, when in the upper viscous layer (region 2) the contribution from the disturbance is of similar magnitude to the Poiseuille component. This will occur when (by (4.19))

$$x = -\frac{1}{6\pi}\ln K + O(1) \tag{4.20}$$

(cf. Smith 1977*b*). So in this region we rescale in the x direction, introducing a new co-ordinate $\tilde{x}$, where

$$x = -\frac{1}{6\pi}\ln K + \tilde{x} \tag{4.21}$$

and the core expansion is now expected to be

$$\left.\begin{aligned} \psi &= \psi_0(y) + K^{-\frac{1}{3}}\psi_1(\tilde{x}, y, t) + \ldots, \\ p &= Kp(\tilde{x}, y, t) + \ldots \end{aligned}\right\} \tag{4.22}$$

[suggested by (4.1), (4.19) and (4.20)]. Here ψ_1 is governed by (3.2) and produces a slip $u_1(\tilde{x}, t) = \Psi_{1y}(y = 0)$ given by

$$u_1(\tilde{x}, t) = \frac{1}{\beta_2^2}\,4\pi hG^*(-2i\pi)\,e^{2\pi\tilde{x}} \tag{4.23}$$

and so we introduce a boundary layer of thickness $O(K^{-\frac{1}{3}})$ near the wall, defining new variables z, Ψ by

$$\left.\begin{aligned} z &= K^{\frac{1}{3}}y, \\ \Psi &= K^{\frac{2}{3}}\psi = \Psi_0 + O(K^{-\frac{1}{3}}). \end{aligned}\right\} \tag{4.24}$$

Following the usual procedure, from the governing equations it is found that

$$\Psi_0 = u_1 + \tfrac{1}{2}z \tag{4.25}$$

and so an inner layer is required (in order that the slip may be reduced to zero) where

$$\left.\begin{aligned} \hat{\Psi} &= K\psi = K^{\frac{1}{3}}\Psi = \hat{\Psi}_0 + O(K^{-\frac{1}{3}}) \\ \hat{z} &= K^{\frac{2}{3}}y = K^{\frac{1}{2}}z. \end{aligned}\right\} \tag{4.26}$$

Then from the Navier–Stokes equations (1.4), $\hat{\Psi}_0$ satisfies the Stokes equation, i.e.

$$\frac{1}{\beta_2^2}\hat{\Psi}_{0\hat{z}t} = \frac{1}{\beta_2^2}\frac{\partial u_1}{\partial t} + \hat{\Psi}_{0\hat{z}\hat{z}\hat{z}}$$

with

$$\left.\begin{aligned} \hat{\Psi}_{0\hat{z}} = \hat{\Psi}_0 = 0 \quad &\text{on} \quad \hat{z} = 0, \\ \hat{\Psi}_{\hat{z}} \to u_1 \quad &\text{as} \quad \hat{z} \to \infty. \end{aligned}\right\} \tag{4.27}$$

Consequently $\hat{\Psi}_0$ may be found using the method used for equation (4.11). We notice that in this lower layer the flow is still dominated by the disturbance caused by the hump. It is not until x is very large and negative (specifically when

$$x = -\frac{1}{3\pi}\ln K + \tilde{x} \tag{4.28}$$

with $\tilde{x} = O(1)$) that the effects of the basic flow and of the distortion become comparable in the lowest layer. This far upstream, the core solution takes on the form

$$\psi = \psi_0(y) + K^{-\frac{2}{3}}\psi_1(\tilde{x}, y, t) + \ldots \tag{4.29}$$

with $\psi_{1y}(y=0)$ given by (4.23). Also we define the boundary-layer variables by

$$\left.\begin{aligned} \Psi &= K^{\frac{4}{3}}\psi = \Psi_0 + K^{\frac{1}{3}}\Psi_1 + \dots, \\ z &= K^{\frac{2}{3}}y, \quad p = K^{\frac{2}{3}}P_1(\tilde{x},t) + \dots \end{aligned}\right\} \tag{4.30}$$

and find, using (1.4) that Ψ_0 satisfies the Stokes-layer equation

$$\frac{1}{\beta_2^2}\Psi_{0zx} = \Psi_{0zzz} + \frac{1}{\beta_2^2}\frac{\partial u_1}{\partial x} \tag{4.31}$$

with boundary conditions $\Psi_0 = \Psi_{0z} = 0$ on $z = 0$,

$$\Psi_{0z} \to u_1 + \tfrac{1}{2}z \quad \text{as} \quad z \to \infty. \tag{4.32}$$

Consequently the boundary layer is driven by the core solution at this distance upstream of the hump. If we split Ψ_0 into steady and unsteady components, i.e.

$$\Psi_0 = \Psi_0^{(s)}(\tilde{x},z) + \Psi_0^{(u)}(\tilde{x},z,t) \tag{4.33}$$

then it is a simple matter to show that $\Psi_0^{(s)} = \frac{1}{4}z^2$ (from the Poiseuille flow), whilst $\Psi_0^{(u)}$ is governed by the Stokes equation (4.31), which again may be solved in the usual fashion.

To summarize, we see that for this regime of β_0, the effect of the hump propagates upstream, and it is not until a distance $-1/3\pi \ln K$ (upstream) that the main (undisturbed) flow asserts its dominance in the boundary layers near the walls of the channel. For oscillatory humps it is at this distance from the hump that the basic and oscillatory components of the flow would first become comparable. Note too that the results of this section, as $\beta_2 \to \infty$, match with those of the previous section as $\beta_1 \to 0$.

5. Discussion

We are now in a position to describe the effects of unsteady walls on an otherwise steady channel flow, for progressively faster wall movements (β_0 descreasing) for distortions of height $O(K^{-\frac{1}{3}})$.

First, suppose that $\beta_0 = O(K^{-\frac{1}{3}})$. Then we see that the steady (Poiseuille) flow and the unsteady (Stokes) flow are inextricably coupled in the boundary-layer problem; for this order of β_0 in general we must solve (see § 2) the nonlinear unsteady boundary-layer equation. For this regime of β_0, the boundary layer drives the core solution, and there is no significant influence upstream of the channel distortion. The numerical results of § 2, with $\beta_0 = K^{-\frac{1}{3}}\beta$, show, however, that the asymptotic form derived (in § 3) for $\beta \to 0$ describes the flow quite reasonably, even for only moderately small values of $\beta(\sim \frac{1}{2})$, with the appearance of a second boundary layer – essentially a Stokes layer of thickness $O(K^{-\frac{1}{3}}\beta)$.

As β_0 becomes progressively smaller, the steady (Poiseuille) flow and the unsteady flow components become progressively more decoupled in the viscous layers, the effect of the unsteadiness dominating. In particular, when β_0 decreases to $O(K^{-\frac{1}{2}})$, appreciable upstream influence first appears in the motion. The core solution then begins to drive the boundary-layer solution. When β_0 decreases still further, to $O(K^{-\frac{2}{3}})$, the unsteady disturbance produces an effect of the same order as the main flow itself in the core (in the boundary layer the unsteadiness dominates completely over the basic flow), at least in the region of the hump. Any further reduction in the order of β_0

would result in unsteadiness dominating in the core as well, although the leading term of the stream function would still be governed by (4.2), however small β_0. Consequently for this size of hump ($O(K^{-\frac{1}{3}})$), we have a complete description of the flow produced over the entire range of β_0, the three regimes of β_0 matching at their respective upper and lower limits.

As noted in the introduction, in any experiment the channel would have to be very long in order that the present analysis would be applicable. We are now in a position to give more details on this. For $\beta_0 = O(K^{-\frac{1}{3}})$ we see from § 2 that the perturbation pressure is $O(K^{\frac{1}{3}})$. This suggests that in any experiment we must have channels of length $\gg O(K^{\frac{1}{3}})$ in order that at the channel ends the driving pressure dominates over the perturbation pressure. In § 3 this requirement is increased to $\gg O(K^{\frac{2}{3}})$ and in § 4 is increased still further to $\gg O(K)$. We therefore see, as the wall motion becomes increasingly faster, that longer and longer channels are required in order that the analysis of this paper applies. A further experimental requirement, in order that the flow upstream be steady, is that the impedance of the upstream portion of the channel is considerably greater than that of the downstream part, i.e. the distortion should be sited such that the upstream portion of the channel is larger than the downstream portion. This would then ensure that the flow-rate fluctuations will be transmitted downstream rather than upstream, as required.

Finally, note that intermediate orders of β_0 may be described by either the higher or lower orders of β_0 considered in this paper, the asymptotic expansions given being commutative.

The author wishes to thank Dr F. T. Smith for suggesting the problem, and for many useful discussions. The financial support of the Science Research Council is also gratefully acknowledged. Also the referees are thanked for their suggestions on the presentation of this paper.

REFERENCES

SMITH, F. T. 1974 *J. Inst. Math. Appl.* **13**, 127.

SMITH, F. T. 1976*a* *Q. J. Mech. Appl. Math.* **29**, 343.

SMITH, F. T. 1976*b* *Q. J. Mech. Appl. Math.* **29**, 365.

SMITH, F. T. 1977 *J. Fluid Mech.* **79**, 631.

SMITH, F. T. 1978 *J. Inst. Math. Appl.* **21**, 145.

STEWARTSON, K. & WILLIAMS, P. G. 1969 *Proc. Roy. Soc.* A **312**, 181.

TILLET, J. P. K. 1968 *J. Fluid Mech.* **32**, 273.